

Spatial Entanglement of Formation in Thermal States of One or Two Identical Non-Interacting Massive Bosons

R.A.W. Bradford

Received: 21 February 2009 / Accepted: 15 April 2009 / Published online: 23 April 2009
© Springer Science+Business Media, LLC 2009

Abstract The entanglement of formation (EoF) between one-dimensional spatial regions is calculated for one and two identical, non-interacting, non-relativistic bosons. Thermal states are approximated by mixtures of up to 13 energy eigenstates. The EoF is found to diminish as inverse temperature to a power of ~ 0.62 in one spatial dimension.

Keywords Entanglement of formation · Bosons · Thermal state

1 Introduction

The entanglement of quantum systems has been a vigorous area of research for the last fifteen years. This has been stimulated by the realisation that entanglement is the essential ingredient in many applications in quantum communication, [1], quantum teleportation, [2], quantum cryptography, [3–5], and quantum computing [6, 7]. However, a motivation of longer standing is the appreciation that entanglement is necessary for the logical coherence of quantum mechanics. The resolution of the EPR problem, [8], is the archetypal example.

Entanglement is not an intrinsic property of a quantum system, as emphasised in [9, 10]. Entanglement exists only with respect to a given partition of the system into component parts. Specifically it must be possible to express the Hilbert space in question as the direct product of the Hilbert spaces of constituents, $H = H_A \otimes H_B$. With respect to this particular partition a given pure state is said to be separable if and only if it can be written as the direct product of A and B states, i.e., $|\psi\rangle = |a\rangle_A \otimes |b\rangle_B$, where $|a\rangle_A \in H_A$ and $|b\rangle_B \in H_B$. A state which cannot be so factorised is said to be entangled with respect to the partition $H = H_A \otimes H_B$.

A possible partition is the spatial partition which results from the field description. In this partition the objects whose states form the component parts are not the particles but spatial regions. Spatial entanglement of this sort arises naturally below the BEC transition temperature, [11–16], essentially because of the dominance of a single energy eigenstate.

R.A.W. Bradford (✉)
1 Merlin Haven, Wotton-under-Edge, Glos., GL12 7BA, UK
e-mail: RickatMerlinHaven@hotmail.com

Clearly, there can be no entanglement with respect to a partition into particles when only one particle is present. However, the partition into spatial regions is just as valid for one particle as for many, so the potential for spatial entanglement exists for one particle systems, [9, 17]. The suggestion that the spatial entanglement of single particle systems should be experimentally detectable probably remains controversial, criticisms of early proposals being given in [18–20]. However, schemes to detect single particle and/or spatial entanglement unambiguously continue to be devised and attempted, e.g. [21–25], but are so far probably not free of loopholes.

Quantification of the degree of entanglement has been widely discussed, e.g., [26–30]. Many different measures are available, but often present computational difficulties, especially for mixed states. Whilst spatial entanglement in systems of free bosons has been calculated before, e.g. [11–16], this has been restricted to quantification via the negativity, [15, 31], or by purity measures, [14, 27]. In effect these entanglement witnesses are restricted to quantifying the entanglement of just a single mode, and hence are all of order unity or less despite the many-particle systems considered. In contrast, here we calculate the entanglement of formation (EoF, [32]). This is the original feature of this paper.

The definition of the EoF (given in the [Appendix](#)) is uncontentious but unfortunately provides difficulties as regards explicit computation in the general case for mixed states. A closed form expression for the EoF has been given in [33, 34] for the case of an arbitrary mixture of two qubits. Simple expressions have also been found for isotropic states (the class of density matrices which are convex mixtures of a maximally entangled state and the maximally mixed state), [35]. However, the general case remains a challenge to evaluate. In this paper, the EoF has been evaluated by numerical optimisation (the details of which are described in the [Appendix](#)). The complexity of the computation of the EoF causes attention to be restricted to small numbers of particles and states. Nevertheless, we evaluate the spatial EoF for thermal states of one and two non-relativistic, non-interacting bosons. The thermal states are defined as mixtures of up to 13 energy eigenstates of a confining ‘box’ potential. The calculations are restricted to the 1D case.

2 Formulation of Partitioned States

Numerical examples will be restricted to the 1D case and hence the formulation below is also restricted to 1D, though it generalises to 3D in a straightforward manner. We consider non-relativistic, non-interacting bosons confined either through some central potential or within a box. The energy eigenfunctions of the Hamiltonian, $\hat{H} = -\hbar^2 \partial_x^2 / 2m + V(x)$, are denoted $u(n, x)$. The potential is assumed to produce an infinite set of bound state eigenfunctions which are orthonormal and complete. Examples include a harmonic potential or box confinement. The latter case will be used in numerical examples, although not necessary for the general development. We shall refer to the total spatial region as a ‘box’ for convenience, but this may be infinite space. The true box modes are $u(n, x) = \sqrt{\frac{2}{L}} \sin(\frac{n\pi x'}{L})$, where $x' = x + L/2$, which vanish at the box walls, $x = \pm L/2$.

In terms of a Fock basis, a quantum field operator is $\hat{\psi}(x) = \sum_{n=1}^{\infty} u(n, x) \hat{a}_n$. Formulation of the partitioned states broadly follows [11]. The creation operator for a mode specified by $f(x)$ can be written $\hat{f}^+ = \int_{Box} f(x) \hat{\psi}^+(x) dx$ and f is assumed normalised, $\int_{Box} |f(x)|^2 dx = 1$. A normalised state of a single particle in this mode is then $\hat{f}^+ |0\rangle$. Now consider the box to consist of two spatial partitions, labelled A and B . For region A , the

mode function is modified such that its support is A . Hence the creation operator for a particle in this mode, and hence in region A , is \hat{f}_A^+ , where,

$$\alpha \hat{f}_A^+ = \int_{x \in A} f(x) \hat{\psi}^+(x) dx. \tag{1}$$

The constant, α , is defined so that $\hat{f}_A^+|0\rangle$ is a normalised state representing a single particle in this mode in region A . Hence we require, $|\alpha|^2 = \int_{x \in A} |f(x)|^2 dx$. Creation operators for region B are defined analogously. Now choosing $f(x) = u(n, x)$, we have,

$$\hat{f}^+ \rightarrow \hat{a}_n^+ = \alpha_n^A \hat{a}_{An}^+ + \alpha_n^B \hat{a}_{Bn}^+ + \alpha_n^O \hat{a}_{On}^+, \tag{2}$$

where,

$$\hat{a}_{An}^+ = \frac{1}{\alpha_n^A} \sum_{k=1}^{\infty} R_{nk}^A \hat{a}_k^+ \tag{3}$$

and,

$$R_{nk}^A \equiv \int_{x \in A} u(n, x) u(k, x)^* dx, \tag{4}$$

and,

$$|\alpha_n^A|^2 = \sum_{k=1}^{\infty} |R_{nk}^A|^2 = \int_{x \in A} |u(n, x)|^2 dx. \tag{5}$$

The latter expression follows from the completeness relation for the eigenfunctions, $\sum_{k=1}^{\infty} u(k, x)^* u(k, y) = \delta(x - y)$, which also gives $\sum_{k=1}^{\infty} R_{mk}^{A*} R_{nk}^A = R_{nm}^A$. Equation (5) also holds for the B region. The commutation relations between the partitioned creation and annihilation operators are,

$$[\hat{a}_{An}^+, \hat{a}_{Ak}^+] = [\hat{a}_{An}^+, \hat{a}_{Bk}^+] = [\hat{a}_{An}^+, \hat{a}_{Ak}] = [\hat{a}_{An}, \hat{a}_{Bk}] = [\hat{a}_{Am}, \hat{a}_{Bn}^+] = 0. \tag{6}$$

The last of these follows from $\int_{x \in A} dx \int_{y \in B} dy \cdot u_n(x) u_m(y)^* \delta(x - y) \equiv 0$. However, the distinction between the partitioned operators and the true Fock operators results from the final commutator,

$$S_{nm}^A \equiv [\hat{a}_{An}, \hat{a}_{Am}^+] = \frac{1}{\alpha_n^{A*} \alpha_m^A} \sum_{k=1}^{\infty} R_{nk}^{A*} R_{mk}^A = \frac{R_{mn}^A}{\alpha_n^{A*} \alpha_m^A}. \tag{7}$$

This is unity when $n = m$, i.e. $S_{nn}^A = 1$, consistent with Fock space, $[\hat{a}_m, \hat{a}_n^+] = \delta_{nm}$. However, unlike the latter, (7) is also non-zero in general for $n \neq m$. It is this latter fact that gives the partition its non-trivial structure and leads to the entanglement of formation falling below its maximum possible value in certain cases. The Fock states for the whole box are,

$$|N_1(k_1), N_2(k_2), \dots\rangle \equiv \frac{(\hat{a}_{k_1}^+)^{N_1}}{\sqrt{N_1!}} \cdot \frac{(\hat{a}_{k_2}^+)^{N_2}}{\sqrt{N_2!}} \dots |0\rangle. \tag{8}$$

Analogously we can define partitioned states with respect to the A and B regions by,

$$\xi |N_1(k_1), N_2(k_2), \dots\rangle_A \equiv \frac{(\hat{a}_{Ak_1}^+)^{N_1}}{\sqrt{N_1!}} \cdot \frac{(\hat{a}_{Ak_2}^+)^{N_2}}{\sqrt{N_2!}} \dots |0\rangle \tag{9}$$

and similarly with A replaced by B . However, caution is needed when dealing with these partitioned states since they are not all mutually orthogonal. Indeed, they would not all be normalised, either, were it not for the introduction of the ξ coefficient. Partitioned states of N particles all in the same energy eigenstate, k , i.e.,

$$|N(k)\rangle_A \equiv \frac{(\hat{a}_{Ak}^+)^N}{\sqrt{N!}} \cdot |0\rangle \tag{10}$$

are normalised and mutually orthogonal. Hence, $\xi = 1$ in these cases. However, the partitioned states of two or three particles of differing energy require $\xi > 1$ in order to be normalised in general. For the states $|nm\rangle_A \equiv |1(n), 1(m)\rangle_A$ and $|nmq\rangle_A \equiv |1(n), 1(m), 1(q)\rangle_A$, where n, m and q are all different, normalisation requires $|\xi_{nm}^A|^2 = \langle 0|\hat{a}_{Am}\hat{a}_{An}\hat{a}_{An}^+\hat{a}_{Am}^+|0\rangle$ and $|\xi_{nmq}^A|^2 = \langle 0|\hat{a}_{Aq}\hat{a}_{Am}\hat{a}_{An}\hat{a}_{An}^+\hat{a}_{Am}^+\hat{a}_{Aq}^+|0\rangle$. Repeated use of the commutation relation, (7), leads to,

$$|\xi_{nm}^A|^2 = 1 + |S_{nm}^A|^2, \tag{11}$$

$$|\xi_{nmq}^A|^2 = 1 + 2\Re(S_{nm}^A S_{nq}^A S_{mq}^A) + [|S_{nm}^A|^2 + |S_{nq}^A|^2 + |S_{mq}^A|^2]. \tag{12}$$

Two single-particle partitioned states in different energy states, $|n\rangle_A \equiv |1(n)\rangle_A$ and $|m\rangle_A \equiv |1(m)\rangle_A$, are not orthogonal in general. In fact,

$${}_A\langle n|m\rangle_A = \langle 0|[\hat{a}_{An}, \hat{a}_{Am}^+]|0\rangle = S_{nm}^A. \tag{13}$$

Similarly, a pair of two-particle states, say $|nq\rangle_A$ and $|nm\rangle_A$, will not in general be orthogonal, as reduction of ${}_A\langle nm|nq\rangle_A = \langle 0|\hat{a}_{Am}\hat{a}_{An}\hat{a}_{An}^+\hat{a}_{Aq}^+|0\rangle$ using the commutation relations shows. All the above relations apply equally with region A replaced by B . Partitioned states for one region are all orthogonal to partitioned states for another region. Partitioned states of N particles are orthogonal to any partitioned state of a differing number of particles.

3 Single Particle Orthogonalisation Procedure

Hereafter we shall assume that the regions A and B are each half of the box. For a pure energy eigenstate the EoF would then be unity. The density matrix for a mixture of N_S single particle energy eigenstates n_1, n_2, \dots is,

$$\hat{\rho} = \sum_{i=1}^{N_S} p_i |n_i\rangle\langle n_i|. \tag{14}$$

Each single particle energy eigenstate can be written in the form,

$$|n_j\rangle = \alpha_{n_j}^A |n_j\rangle_A |0\rangle_B + \alpha_{n_j}^B |0\rangle_A |n_j\rangle_B, \tag{15}$$

$$|\alpha_{n_j}^{A,B}|^2 = \int_{x \in A,B} |u(n_j, x)|^2 dx. \tag{16}$$

We have written (15) with arbitrary α coefficients but we consider only $|\alpha_j^{A,B}|^2 = 1/2$ in the numerical examples, i.e. the box is partitioned into equal halves. Because the partitioned

states $\{|n_j\rangle_{A,B}\}$ are not orthonormal, we need to introduce an orthonormalizing scheme before attempting to find the EoF numerically. The orthonormalized single-particle A -partition states are denoted $\{|\psi_j^A\rangle\}$. In terms of these the $|n_j\rangle_A$ states are written,

$$|n_j\rangle_A = \sum_{k=1}^j C_{jk}^A |\psi_k^A\rangle. \tag{17}$$

Similarly, the B -system states are written $|n_j\rangle_B = \sum_{k=1}^j C_{jk}^B |\psi_k^B\rangle$. The first of the basis vectors is just,

$$|\psi_1^{A,B}\rangle = |n_1\rangle_{A,B}. \tag{18}$$

For $j > 1$, orthonormality gives the first coefficient in (17) as,

$$C_{j1}^A = {}_A\langle n_1 | n_j \rangle_A = S_{[1j]}^A \tag{19}$$

where for clarity we have introduced the notation $S_{[pq]}^A$ to stand for S_{KL}^A evaluated at $K = n_p$ and $L = n_q$. The remaining coefficients are found by successively forming the scalar product of (17) with each state $|\psi_k^A\rangle$ in turn. This leads to the following general expression which applies for $1 < k < j$,

$$C_{jk}^A = \frac{1}{C_{kk}^{A*}} \left[S_{[kj]}^A - \sum_{i=1}^{k-1} C_{ki}^{A*} C_{ji}^A \right]. \tag{20}$$

The last coefficient for each ‘ j ’ is given by,

$$C_{jj}^A = \sqrt{1 - \sum_{k=1}^{j-1} |C_{jk}^A|^2}. \tag{21}$$

Note that (20) involves finding the k th coefficient for the j th state in terms of, (a) the i th coefficients of the j th state, with $i < k$ and which have thus already been found, and, (b) the coefficients for the k th states with $k < j$, which have also already been found. Thus the only additional evaluation required for each new C_{jk}^A is the scalar product $S_{[kj]}^A$ from (4), (5), (7). Equations (19)–(21) apply equally with A replaced throughout by B .

The orthonormalization scheme of (17)–(21) results in the N_S energy states, (15), being expressible in terms of $N_S + 1$ A -system states and $N_S + 1$ B -system states. These states are the A -vacuum, $|0\rangle_A$, and the N_S occupied A -states, $|\psi_j^A\rangle$, plus the B -system equivalents. Hence, the density matrix for a mixture of N_S distinct energy states is a special case of an $(N_S + 1) \times (N_S + 1)$ bipartite density matrix.

4 Mixtures Approximating the Thermal State of a Single Particle

In this section we consider single particle mixtures of the first ten consecutive energy states, resulting in a density matrix of dimension 121. The probabilities are chosen to approximate a thermal state at temperature T , and a range of values of E_1/kT are analysed from 0.001 to 2 (where E_1 is the ground state energy and k is Boltzmann’s constant). Because we are using only 10 energy states, the mixture ceases to be an accurate representation of the thermal state when more than 10 states would contribute significantly to the true thermal mixture.

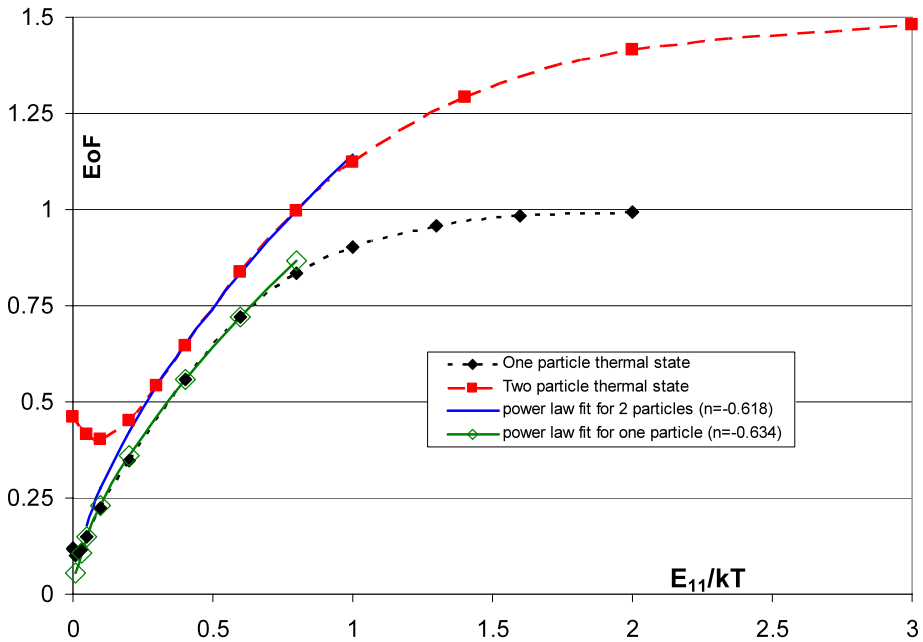


Fig. 1 EoF for thermal states of one and two bosons compared. The representation of the thermal state becomes poor for $E_1/kT < 0.03$ for one particle, and for $E_{11}/kT < 0.2$ for two particles, but the extrapolation to zero entanglement at high temperature is clear (as illustrated by the T^{-n} fits)

The true thermal mixture would have probabilities relative to that of the ground state given by the Boltzmann factor,¹

$$\frac{p_n}{p_1} = \exp \left\{ -\frac{E_1}{kT} (n^2 - 1) \right\}. \tag{22}$$

This is used as the basis for our assumed probabilities. However, the normalisation is adjusted to ensure the probabilities sum to unity over just the first 10 states. The approximation to the thermal state is expected to be reasonable for $kT \leq 30E_1$, for which the smallest contributing probability (p_{10}) is $\leq 5\%$ of the largest (p_1).

The EoF was found using the numerical method described in the [Appendix](#) and the result for each temperature is shown in [Fig. 1](#) (black curve) and in [Table 1](#). A surprise is that the case of equal probabilities ($E_1/kT = 0$) does not produce the minimum EoF. Actually the minimum EoF occurs for the unequal probabilities labelled $E_1/kT = 0.01$, see [Table 1](#), for which p_1 exceeds p_{10} by about $\times 2.7$ (though this case is not a good representation of a thermal state).

However, for $E_1/kT \geq 0.03$, for which the approximation to the thermal state is good, the behaviour of the EoF is as expected. At temperatures $kT < E_1/2$ the thermal state approximates to just ground state occupation, and hence the EoF becomes unity. However, at higher temperatures the EoF reduces steadily. [Figure 1](#) suggests that the EoF is tending towards zero at high temperature—until the use of only 10 states limits the accuracy of the

¹Since we are considering states of just one particle the Bose distribution is not appropriate.

Table 1 Entanglement of 10-state mixtures approximating the thermal state of a single particle at various temperatures (50/50 partition)

E_1/kT	EoF
0	0.1217
0.001	0.1184
0.01	0.1020
0.03	0.1167
0.05	0.1492
0.1	0.2235
0.2	0.3471
0.4	0.5578
0.6	0.7211
0.8	0.8331
1	0.9035
1.3	0.9591
1.6	0.9831
2	0.9949

representation of the thermal state. A power law fit suggests $EoF \propto T^{-0.63}$ for one particle in 1D when kT is sufficiently larger than E_1 .

5 The EoF of Two-Particle Thermal States

Consideration is restricted to mixtures of just 13 two-particle energy states, namely the states whose energy quantum numbers are (1, 1), (1, 2), (1, 3), (1, 4), (1, 5), (2, 2), (2, 3), (2, 4), (2, 5), (3, 3), (3, 4), (3, 5) and (4, 4). This includes all states whose energy is 17 times the ground state, (1, 1), energy or less. The density matrix is,

$$\hat{\rho} = \sum_{n,m} p_{nm} |n, m\rangle \langle n, m| \tag{23}$$

where (n, m) is summed over the 13 values indicated above. The probabilities, p_{nm} , are defined by the Boltzmann distribution,

$$\frac{p_{nm}}{p_{11}} = \exp \left\{ -\frac{E_1}{kT} \left(\frac{n^2 + m^2}{2} - 1 \right) \right\}. \tag{24}$$

The probabilities are renormalized so that they sum to unity over the 13 states considered. It is expected that temperatures up to $kT/E_{11} \sim 5$ should be well represented by just 13 states, for which the smallest contributing probability (p_{12}) is $\leq 4\%$ of the largest (p_1). For higher temperatures our 13-state mixture will depart from the true thermal state. Each of the 13 pure two-particle states can be expressed in terms of partitioned states in one of two ways, depending upon whether $n = m$ or $n \neq m$, thus,

$$n = m: \quad |nn\rangle = \frac{1}{2} [|0\rangle_A |nn\rangle_B + \sqrt{2} |n\rangle_A |n\rangle_B + |nn\rangle_A |0\rangle_B], \tag{25}$$

$$n \neq m: \quad |nm\rangle = \frac{1}{2} [\xi_{nm} \{ |0\rangle_A |nm\rangle_B + |nm\rangle_A |0\rangle_B \} + |n\rangle_A |m\rangle_B + |m\rangle_A |n\rangle_B]. \tag{26}$$

The main task we have in formulating the problem is to carry out the orthonormalizing process. This is required for both the one-particle partitioned states, $|n\rangle_{A,B}$, and also the two particle partitioned states, $|nm\rangle_{A,B}$, since neither are orthonormal as they stand. The five one-particle states, $\{|i\rangle_A, i = 1, 2, \dots, 5\}$, are orthonormalized precisely as described previously, the orthonormalized set of states being denoted $\{|\psi_i^A\rangle, i = 1, 2, \dots, 5\}$, where $|\psi_1^A\rangle \equiv |1\rangle_A$ and the remaining states are defined as in Sect. 3. Because (25), (26) involve sums of products of one particle states, the numerical coefficients which finally appear are obtained as sums of products of the $C_{jk}^{A,B}$ coefficients of Sect. 3.

Orthonormalization of the two-particle states is similar. There are 13 two-particle states for each partition, $|11\rangle_A, |12\rangle_A, |13\rangle_A, |14\rangle_A, |15\rangle_A, |22\rangle_A, |23\rangle_A, |24\rangle_A, |25\rangle_A, |33\rangle_A, |34\rangle_A, |35\rangle_A, |44\rangle_A$. These are to be expressed in terms of the orthonormalized states $\{|\theta_I^A, I = 1, 2, \dots, 13\}$, where $|\theta_1^A\rangle \equiv |11\rangle_A$, via the definitions,

$$|ij\rangle_A = \sum_{K=1}^J D_{JK}^A |\theta_K^A\rangle \tag{27}$$

where the capital indices take values in the range $1, 2, \dots, 13$, labelling the two-particle states, and state J denotes (ij) . With this notation, the D -coefficients are found from a similar formula to (20), i.e.,

$$\text{for } 1 < K < J, \quad D_{JK}^A = \frac{1}{D_{KK}^{A*}} \left[\langle K|J\rangle_A - \sum_{I=1}^{K-1} D_{KI}^{A*} D_{JI}^A \right], \tag{28}$$

$$\text{for } K = 1, \quad D_{J1}^A = {}_A\langle 1|J\rangle_A \tag{29}$$

where the two-particle scalar products, ${}_A\langle K|J\rangle_A$, are found from formulae depending upon which quantum numbers are common, i.e.,

$${}_A\langle nm|pq\rangle_A = [S_{np}^A S_{mq}^A + S_{nq}^A S_{mp}^A] / \xi_{nm} \xi_{pq}, \tag{30}$$

$${}_A\langle nm|nq\rangle_A = [S_{mq}^A + S_{nm}^A S_{nq}^A] / \xi_{nm} \xi_{nq}, \tag{31}$$

$${}_A\langle nm|qq\rangle_A = \sqrt{2} S_{nq}^A S_{mq}^A / \xi_{nm}, \tag{32}$$

$${}_A\langle nq|qq\rangle_A = \sqrt{2} S_{nq}^A / \xi_{nq}, \tag{33}$$

$${}_A\langle nn|qq\rangle_A = (S_{nq}^A)^2. \tag{34}$$

These expressions all follow from the commutation relations, (7). The final coefficient is determined by normalisation,

$$D_{JJ}^A = \sqrt{1 - \sum_{K=1}^{J-1} |D_{JK}^A|^2}. \tag{35}$$

After some labour, the components of the density matrix, (23), can thus be found in terms of the orthonormal basis formed by the direct product of the 19 A -partition states, $|0\rangle_A, \{|\psi_i^A\rangle, i = 1, 2, \dots, 5\}, \{|\theta_I^A, I = 1, 2, \dots, 13\}$, with the B -partition equivalents. The resulting density matrix is of dimension $19 \times 19 = 361$, though its rank is, of course, only 13.

Table 2 Entanglement of 13-state mixtures approximating the thermal state of two particles at various temperatures (50/50 partition)

E_{11}/kT	EoF
$p = 1/13$	0.4613
0.05	0.4147
0.1	0.4020
0.2	0.4504
0.3	0.5436
0.4	0.6457
0.6	0.8372
0.8	0.9966
1.0	1.1226
1.4	1.2911
2.0	1.4148
3.0	1.4809
∞	1.5

The EoF of thermal mixtures of these 13 two-particle energy eigenstates has been found using the numerical procedure described in the [Appendix](#). The results are shown plotted against inverse temperature in [Fig. 1](#) and compared with the EoF of the one-particle thermal states. The salient feature is that the EoF reduces with increasing temperature, at least so long as $E_{11}/kT > 0.2$ when the representation of the thermal state is good.

Like the one particle case, a surprise is that the case of equal probabilities ($E_{11}/kT = 0$) does not produce the minimum EoF. Actually the minimum EoF occurs for the unequal probabilities labelled $E_{11}/kT = 0.1$, see [Table 2](#), for which p_1 exceeds the smallest probability, p_{12} , by about $\times 5$ (though this case is not a good representation of a thermal state).

[Figure 1](#) shows that the EoF of the two-particle thermal state approaches 1.5 at low temperatures when the mixture becomes the pure ground state. It is easily checked that this is the correct result for a pure state of two identical bosons in the same state.² Comparison with the one-particle thermal state shows that the EoF is larger for two particles (at a given temperature). As the temperature is increased the EoF reduces steadily (until $E_{11}/kT < 0.2$ when the representation of the thermal state becomes poor). A power law fit suggests $\text{EoF} \propto T^{-0.62}$ for two particles in 1D when kT is sufficiently larger than E_{11} . This dependence on temperature is almost identical to the one-particle result of [Sect. 3](#).

Appendix: Definition and Numerical Determination of the EoF

For pure quantum states of a composite system, the entanglement of formation is defined as the von Neumann entropy of the reduced density matrix of one component part. Thus, if $|\psi\rangle$ is the state of the composite system, then $\text{EoF} = S_{vN}(\hat{\rho}_A)$, where $\hat{\rho}_A = \text{Tr}_B(|\psi\rangle\langle\psi|) = \sum_{b \in B} \langle b|\psi\rangle\langle\psi|b\rangle$, where A and B are the components parts, and $S_{vN}(\hat{\rho}_A) \equiv$

²For N bosons in the same energy state a good approximation to the EoF for a 50/50 partition is $1 + \log_2 \sqrt{N}$. This provides an upper bound to the spatial EoF which can be obtained from a BEC. For example, a million atoms in the condensed phase produce an EoF of only 11 ebits. The spatial EoF for N identical bosons in a pure state with differing energies always exceeds that for equal energies. The upper bound for the spatial EoF of N bosons in a pure state with differing energies is N ebits, which contrasts sharply with the EoF for equal energies. The upper bound of N ebits is realised in the case of states of equal parity and a 50–50 partition.

$-\text{Tr}[\hat{\rho}_A \log_2 \hat{\rho}_A]$. Note that we use \log_2 in the definition of entanglement throughout this paper, rather than adopting a varying base according to the dimension of the Hilbert space, as do some authors. The unit of entanglement is that of a two qubit Bell state, or singlet state (one ebit).

The EoF may be easy to evaluate directly from its definition for any explicitly defined pure quantum state. However, the situation is different for mixed states. The density matrix, $\hat{\rho}$, defining a mixed state will have many possible decompositions into explicit mixtures of pure states, $|\psi_i\rangle$. That is, there will be many ways in which to express the density matrix as $\hat{\rho} = \sum_i p_i |\psi_i\rangle\langle\psi_i|$, where the p_i are real probabilities in the range $[0, 1]$ and the states $|\psi_i\rangle$ are normalised but otherwise arbitrary and need not be orthogonal or linearly independent. The average entanglement of this specific decomposition is defined as the average of the entanglements of its pure states, $E_{av} = \sum_i p_i \text{EoF}(|\psi_i\rangle)$. But the value of E_{av} depends upon the decomposition, and hence cannot be the true entanglement in general, since this depends only upon the density matrix and the chosen partition. The entanglement of formation is defined as the minimum value of E_{av} for any decomposition, $\text{EoF} = \text{MIN}_{\{|\psi_i\rangle\}}(E_{av})$. Hence, to find the EoF requires this minimization problem to be solved.

The method of conjugate gradients was used. The particular procedure employed has been described in [36, 37]. The method relies upon all possible decompositions, $\hat{\rho} = \sum_j p'_j |\phi_j\rangle\langle\phi_j|$, of a given density matrix being expressible in terms of a right-unitary transformation from some arbitrary initial decomposition, $\hat{\rho} = \sum_i p_i |\psi_i\rangle\langle\psi_i|$. In these expressions j runs from 1 to J whereas i runs from 1 to I where $J \geq I$. The values of I or J are the cardinalities of the particular decompositions. Thus, there exists a right-unitary matrix U which connects the two decompositions, $|\phi_j\rangle = \sum_{i=1}^I U_{ji} |\tilde{\psi}_i\rangle$, where $U^+U = 1_{I \times I}$ and the tilde on the states denotes that these are the sub-normalized states defined by $|\tilde{\psi}_i\rangle = \sqrt{p_i} |\psi_i\rangle$, $|\tilde{\phi}_i\rangle = \sqrt{p'_i} |\phi_i\rangle$. To capture all possible decompositions the initial decomposition is taken to have cardinality equal to the rank of $\hat{\rho}$, i.e., $I = r$. Parameterizing all right-unitary matrices in some convenient manner thus provides a parameter space whose points are in one-to-one correspondence with the set of all possible decompositions. In our formulation we preferred to search a space of fixed cardinality, starting with a decomposition defined by r non-zero vectors plus ‘padding’ by the required number of additional zero vectors. (All ‘ J ’ vectors will subsequently become non-zero in general). The possibility of improved minima of different cardinality was explored by running the program separately for different cardinalities. The advantage of this is that the matrices, U , are then square, and hence unitary, and can be expressed in terms of an Hermitian matrix, Θ , as $U = \exp(i\Theta)$.

The problem is to find a point in this parameter space which minimises $E_{av} = \sum_i p'_i \text{EoF}(|\phi_i\rangle)$. The basic strategy is to evaluate the gradient of E_{av} in parameter space and then to move in parameter space such that E_{av} reduces as quickly as possible. The obvious algorithm, to move along the negative gradient, produces the method of steepest descents. The method of conjugate gradients is a refinement of this which generally improves the rate of convergence. The expression for the gradient of E_{av} was taken from [37], (10), which gives,

$$dE_{av} = \sum_{i,j} g_{ji} d\Theta_{ij}, \quad \text{where, } g_{ji} = i \text{Tr}_A \{ [\log_2(\hat{\rho}_j^A) - \log_2(\hat{\rho}_i^A)] \text{Tr}_B(|\tilde{\phi}_j\rangle\langle\tilde{\phi}_i|) \} \quad (\text{A.1})$$

where $\hat{\rho}_i = |\phi_i\rangle\langle\phi_i|$, $\hat{\rho}_i^A = \text{Tr}_B(\hat{\rho}_i)$ and $\text{Tr}_{A,B}$ represent tracing-out the states of the indicated partition, e.g. $\text{Tr}_B(\dots) \equiv \sum_{x=B\text{-states}} \langle x | \dots | x \rangle_B$. Note that the gradient matrix, \mathbf{g} , is evaluated at the current position in parameter space, i.e. in terms of the current (evolving) decomposition, $\{|\phi_j\rangle\}$. The bulk of the computational effort is expended in re-evaluating

the gradient matrix at each new point, since its calculation requires eigenvalue extraction in order to find $\log_2(\hat{\rho}_i^A)$.

Some care is necessary since the $J \times J$ real coordinates of the parameter space are not Θ_{ij} , since these are complex with $\Theta_{ij} = \Theta_{ji}^*$, but rather $\Re(\Theta_{ij})$ for $i \leq j$ and $\text{Im}(\Theta_{ij})$ for $i > j$. Different variants of the conjugate gradient method involve different expressions for the conjugate gradient, specifically by how much it differs from the negative gradient. The Polak-Ribiere variant was employed here. In addition, a ‘restart’ was applied every N steps, with N set to the square of the rank. A ‘restart’ resets the conjugate gradient to the negative gradient. Finally, each step requires the line-minimum along the direction of the current conjugate gradient to be found. For this, Brent’s method was used.

A subtlety is that, for initial states of sufficient symmetry, the first order gradient can lead to only a sub-set of parameter space being explored. For example, if the coefficients of the input states are all real (as they are in this paper) then the above algorithm leads only to states with real coefficients, despite complex coefficients being essential to obtain the true minimum of E_{av} in most cases. In our implementation this problem was overcome by alternating the method of conjugate gradients with a simple search along prescribed curves in parameter space, a crude but effective strategy for symmetry breaking.

The major practical difficulty with non-linear optimisation is the distinction between a global minimum and a local minimum. Algorithms like the conjugate gradient method are attracted to local minima. In general there is no guarantee that this will be the global optimum. However, it has been suggested, [38], that local minima of E_{av} are also global minima. This is a major boon to the numerical determination of the EoF. It is easy to check that a local minimum has been reached, simply by evaluation of the finite differences in all coordinate directions. These should all be positive, but some components tend to be small and negative due to numerical limitations. A convergence parameter can be defined as the ratio of the algebraically smallest finite difference to the average value in all directions. This convergence parameter was of considerable utility in practice, further iterations being made until any negative value became suitably small in magnitude.

In passing we note that in all the cases reported here a cardinality equal to the rank of the density matrix was sufficient to obtain the minimum E_{av} , i.e. an optimal decomposition. This was demonstrated simply by trying larger cardinalities, but these never produced an improved minimum for our states. It is known that this is not always the case. Examples where the EoF is non-zero and the cardinality of the optimal decomposition exceeds the rank have been given in [35] and [36]. The latter example considers the so-called Horodecki 3×3 states, [39], whose rank is 7. The EoF of these states was evaluated numerically in [36]. The minimum was not obtained until a cardinality of 14, twice the rank, was used. We have repeated this exercise to test our numerical routines and confirm this result (and also that the magnitude of the EoF is very small, less than 0.01).

References

1. Nielsen, M.A.: Quantum information theory. PhD dissertation, University of New Mexico (1998). quant-ph/0011036
2. Bennett, C.H., Brassard, G., Crepeau, C., Jozsa, R., Peres, A., Wootters, W.: Teleporting an unknown quantum state via dual classical and EPR channels. *Phys. Rev. Lett.* **70**, 1895–1899 (1993)
3. Bennett, C.H., Brassard, G.: In: Proc. IEEE Int. Conf. on Computers, Systems, and Signal Processing, Bangalore, New York, pp. 175–179 (1984)
4. Ekert, A.: Quantum cryptography based on Bell’s theorem. *Phys. Rev. Lett.* **67**, 661–663 (1991)
5. Bostrom, K., Felbinger, T.: Deterministic secure direct communication using entanglement. *Phys. Rev. Lett.* **89**, 187902 (2002)

6. Jozsa, R.: Entanglement and quantum computation. In: Huggett, S., et al. (eds.) *Geometric Issues in the Foundations of Science*. Oxford University Press, Oxford (1997). [quant-ph/9707034](#)
7. Nielsen, M.A., Chuang, I.L.: *Quantum Computation and Quantum Information*. Cambridge University Press, Cambridge (2000)
8. Einstein, A., Podolsky, B., Rosen, N.: Can the quantum-mechanical description of physical reality be considered complete? *Phys. Rev.* **47**, 777–80 (1935)
9. Terra Cunha, M.O., Dunningham, J.A., Vedral, V.: Entanglement in single particle systems. *Proc. R. Soc. Math. Phys.* **463**, 2277–86 (2007)
10. Tommasini, P., Timmermans, E., de Toledo Piza, A.F.R.: The hydrogen atom as an entangled electron-proton system. *Am. J. Phys.* **66**, 881 (1998)
11. Simon, C.: Natural entanglement in Bose-Einstein condensates. *Phys. Rev. A* **66**, 052323 (2002)
12. Anders, J., Kaszlikowski, D., Lunkes, C., Ohshima, T., Vedral, V.: Detecting entanglement with a thermometer. *New J. Phys.* **8**, 140 (2006)
13. Heaney, L., Anders, J., Kaszlikowski, D., Vedral, V.: Spatial entanglement from off-diagonal long range order in a BEC. *Phys. Rev. A* **76**, 053605 (2007)
14. Heaney, L.: Entanglement in the Bose-Einstein condensate phase transition. Preprint (2007). [arXiv:0711.0942](#)
15. Heaney, L., Anders, J., Vedral, V.: Spatial entanglement of a free bosonic field (2006). [arXiv:quant-ph/0607069](#)
16. Kaszlikowski, D., Keil, A., Wiesniak, M., Willenboordse, F.H.: Spatial entanglement of bosons in thermal equilibrium (2006). [arXiv:quant-ph/0601089](#)
17. Peres, A.: Nonlocal effects in Fock space. *Phys. Rev. Lett.* **74**, 4571 (1995)
18. Greenberger, D.M., Horne, M.A., Zeilinger, A.: Nonlocality of a single photon? *Phys. Rev. Lett.* **75**, 2064 (1995)
19. Santos, E.: Comment on “Nonlocality of a single photon?”. *Phys. Rev. Lett.* **68**, 894 (1992)
20. Vaidman, L.: Nonlocality of a single photon revisited again. *Phys. Rev. Lett.* **75**, 2063 (1995)
21. Bjork, G., Jonsson, P., Sanchez Soto, L.L.: Single-particle nonlocality and entanglement with the vacuum. *Phys. Rev. A* **64**, 042106 (2001)
22. Dunningham, A., Vedral, V.: Nonlocality of a single particle. *Phys. Rev. Lett.* **99**, 180404 (2007)
23. Michler, M., Weinfurter, H., Zukowski, M.: Experiments towards falsification of noncontextual hidden variable theories. *Phys. Rev. Lett.* **84**, 5457 (2000)
24. Heaney, L., Anders, J.: Bell-inequality test of spatial mode entanglement. Preprint 0810.2882 (2008)
25. Hessmo, B., Usachev, P., Heydari, H., Björk, G.: Experimental demonstration of single photon nonlocality. *Phys. Rev. Lett.* **92**, 180401 (2004)
26. Popescu, S., Rohrlich, D.: Thermodynamics and the measure of entanglement. *Phys. Rev. A* **56**, R3319–21 (1997)
27. Vedral, V., Plenio, M.B., Rippin, M.A., Knight, P.L.: Quantifying entanglement. *Phys. Rev. Lett.* **78**, 2275–9 (1997)
28. Adesso, G., Illuminati, F., de Siena, S.: Characterizing entanglement with global and marginal entropic measures. *Phys. Rev. A* **68**, 062318 (2003)
29. Adesso, G., Serafini, A., Illuminati, F.: Determination of continuous variable entanglement by purity measurements. *Phys. Rev. Lett.* **92**, 087901 (2004)
30. Li, D.C., Wang, X.P., Cao, Z.L.: Thermal entanglement in the anisotropic Heisenberg XXZ model with the Dzyaloshinskii-Moriya interaction. *J. Phys., Condens. Matter* **20**, 325229 (2008)
31. Vidal, G., Werner, R.F.: Computable measure of entanglement. *Phys. Rev. A* **65**, 032314 (2002)
32. Bennett, C.H., DiVincenzo, D.P., Smolin, J.A., Wootters, W.K.: Mixed state entanglement and quantum error correction. *Phys. Rev. A* **54**, 3824–3851 (1996)
33. Hill, S., Wootters, W.K.: Entanglement of a pair of quantum bits. *Phys. Rev. Lett.* **78**, 5022–5 (1997)
34. Wootters, W.K.: Entanglement of formation of an arbitrary state of two qubits. *Phys. Rev. Lett.* **80**, 2245–8 (1998)
35. Terhal, B.M., Vollbrecht, K.G.: The entanglement of formation for isotropic states. *Phys. Rev. Lett.* **85**, 2625–8 (2000)
36. Audenaert, K., Verstraete, F., de Moor, B.: Variational characterisations of separability and entanglement of formation. *Phys. Rev. A* **64**, 052304 (2001)
37. Gittings, J.R., Fisher, A.: J An efficient numerical method for calculating the entanglement of formation of arbitrary mixed quantum states of any dimension (2003). [arXiv:quant-ph/0302018](#)
38. Prager, T.: A necessary and sufficient condition for optimal decompositions (2001). [arXiv:quant-ph/0106030](#)
39. Horodecki, P.: Separability criterion and inseparable mixed states with positive partial transposition. *Phys. Lett. A* **232**, 333–9 (1997)